

Single Top Quark Production in $e\gamma$ Collisions and Testing Technicolor Models

Xuelei Wang

*Department of Physics, Tsinghua University, Beijing 100084, China;
Physics Department, Henan Normal University, Xinxiang Henan 453002, China.*

Yu-Ping Kuang Hong-Yi Zhou

*China Center of Advanced Science and Technology (World Laboratory),
P.O.Box 8730, Beijing 100080, China;
Institute of Modern Physics, Tsinghua University, Beijing 100084, China.**

Hua Wang Ling Zhang

*Department of Physics, Tsinghua University, Beijing 100084, China.
(TUIMP-TH-98/91)*

We study the single top quark production process $e^+\gamma \rightarrow t\bar{b}\nu_e$ in various kinds of technicolor models in high energy $e\gamma$ collisions at the future e^+e^- linear colliders. It is shown that if there is certain charged pseudo Goldstone boson (PGB) coupling to $t\bar{b}$, the $t\bar{b}$ -channel PGB contribution is dominant, but the situation is quite different from that in the neutral channel $\gamma\gamma \rightarrow t\bar{t}$ due to the large mass difference between the top quark and the bottom quark. At the DESY linear collider TESLA, the event rates in models with $t\bar{b}$ -channel PGB contributions, such as the top-color-assisted technicolor model, etc. are experimentally measurable. The $e^+\gamma \rightarrow t\bar{b}\nu_e$ process provides a feasible test of technicolor models with $t\bar{b}$ -channel charged PGB contributions.

PACS number(s): 14.65.Ha, 12.15.Lk, 12.60.Nz

I. INTRODUCTION

So far the most unclear part of the standard model (SM) is its symmetry breaking sector. Probing the electroweak symmetry breaking (EWSB) mechanism will be one of the most important tasks at future high energy colliders. Dynamical electroweak symmetry breaking (DEWSB), for example technicolor (TC) type theories, is an attractive idea that it avoids the shortcomings of triviality and unnaturality arising from the elementary Higgs field. The simplest QCD-like extended technicolor (ETC) model [1] leads to a too large oblique correction S parameter [2], and is already ruled out by the recent LEP precision electroweak measurement data [3]- [4]. Various improvements have been made to make the predictions consistent with the LEP precision measurement data and even to give possible dynamical explanation of the heaviness of the top quark, for example the walking TC models [5], the Appelquist-Terning one-family model [6], the multi-scale WTC (MWTC) models [7], the top-color-assisted TC models (TC2) [8] [9], the non-commuting ETC model [10], etc. This kind of DEWSB breaking theory is one of the important candidates of the EWSB

mechanism. Due to the strong interaction nature, it is hard to make precise calculations in such DEWSB theories. However, there are some characteristic features in this kind of models, for instance the prediction of certain pseudo Goldstone bosons (PGB's) in the few hundred GeV region. It is thus interesting to find experimentally measurable processes which are sensitive to the PGB's to test this kind of models.

The top quark is the heaviest particle yet experimentally discovered and its mass 175 GeV [11] is close to the electroweak symmetry breaking scale 246 GeV. Thus processes containing the top quark may be sensitive to the EWSB mechanism, and top quark productions at high energy colliders can be good processes for probing the EWSB mechanism. There have been many papers studying testing new physics via top quark productions at high energy colliders in the literatures. For instance, the model-independent studies in the effective Lagrangian formalism have been given in Refs. [12]- [13], supersymmetric corrections to top quark productions at hadron colliders and electron (photon) linear colliders (LC) have been studied in Ref. [14], top quark pair productions at hadron colliders and photon colliders in various technicolor models have been

studied in Refs. [15]- [16]. Recently, there have been a lot of interest in studying single top quark productions which provides a sensitive measurement of the Wtb coupling [19], and many papers studied single top quark productions in new physics models [20]. In Refs. [15]- [16] it is shown that, in the $t\bar{t}$ productions, once there is a neutral PGB coupling strongly to $t\bar{t}$, the $t\bar{t}$ -channel PGB contribution is large and dominant over all other loop corrections, and thus such processes can be sensitive tests of the neutral PGB effects. In this paper, we shall study the $e^+\gamma \rightarrow t\bar{b}\bar{\nu}_e$ process at the high energy $e\gamma$ colliders in various TC models, and we shall show that this process is sensitive to the $t\bar{b}$ -channel charged PGB effects if there is certain charged PGB(s) coupling strongly to $t\bar{b}^*$. We shall see that the $e^+\gamma \rightarrow t\bar{b}\bar{\nu}_e$ process at the $e\gamma$ colliders based on the LC, especially the DESY TeV Energy Superconducting Linear Accelerator (TESLA), is a feasible test of the charged PGB effects, and *the situation is quite different from that in the neutral $\gamma\gamma \rightarrow t\bar{t}$ channel due to the large mass difference between the top quark and the bottom quark*. Of special interest is the test of the charged top-pion effect in the TC2 models. The recent Fermilab CDF data on $t\bar{t}$ production at the Fermilab Tevatron show that the branching fraction for a top quark decaying into a final state e or μ is consistent with the SM prediction [18]. As has been discussed in Ref. [8] that this means a charged top-pion lighter than the top quark is not favored, and a charged top-pion heavier than the top quark will have a broad width so that it is difficult to detect. Our result shows that the $e^+\gamma \rightarrow t\bar{b}\bar{\nu}_e$ process at the DESY TESLA provides a possible test of the charged top-pion effect.

This paper is organized as follows. In Sec. II, we shall present the calculations of the $e^+\gamma \rightarrow t\bar{b}\bar{\nu}_e$ production amplitudes in several currently improved TC models. We take the TC2 model as a typical example of models containing charged PGB's strongly coupling to $t\bar{b}$. The numerical results of the cross sections will be presented in Sec. III, and Sec. IV is a concluding remark.

II. THE $e^+\gamma \rightarrow t\bar{b}\bar{\nu}_e$ PRODUCTION AMPLITUDES

The tree-level SM contributions to the process

$$e^+ + \gamma \rightarrow t + \bar{b} + \bar{\nu}_e \quad (1)$$

are shown in Fig.1(a-d). The momenta of these particles will be denoted by p_{e^+} , p_γ , p_t , $p_{\bar{b}}$ and $p_{\bar{\nu}}$, respectively. In high energy processes, the effects of m_e is negligibly small. Thus we neglect it in the following calculations. We take the unitary gauge. The obtained tree-level SM amplitude is explicitly

$$\mathcal{M}_0 = \mathcal{M}_0^{(a)} + \mathcal{M}_0^{(b)} + \mathcal{M}_0^{(c)} + \mathcal{M}_0^{(d)}, \quad (2)$$

where

$$\begin{aligned} \mathcal{M}_0^{(a)} = & -\frac{8i\sqrt{2\pi\alpha}M_W^2G_F}{6}G(p_{\bar{b}} - p_\gamma; m_b) \\ & G(p_{e^+} - p_{\bar{\nu}}; M_W)\bar{u}_t\gamma_\mu L(p_{\bar{b}} - p_\gamma + m_b)\not{p}_{\nu_b} \\ & T_{\mu\lambda}(p_{e^+} - p_{\bar{\nu}})\bar{v}_e\gamma_\lambda Lv_{\nu_e}, \end{aligned} \quad (3)$$

$$\begin{aligned} \mathcal{M}_0^{(b)} = & -\frac{8i\sqrt{2\pi\alpha}M_W^2G_F}{3}G(p_t - p_\gamma; m_t) \\ & G(p_{e^+} - p_{\bar{\nu}}; M_W)\bar{u}_t\not{p}_t(p_t - p_\gamma + m_t)\gamma_\mu Lv_b \\ & T_{\mu\lambda}(p_{e^+} - p_{\bar{\nu}})\bar{v}_e\gamma_\lambda Lv_{\nu_e}, \end{aligned} \quad (4)$$

$$\begin{aligned} \mathcal{M}_0^{(c)} = & -\frac{8i\sqrt{2\pi\alpha}M_W^2G_F}{2}G(p_{e^+} + p_\gamma; 0) \\ & G(p_t + p_{\bar{b}}; M_W)\bar{u}_t\gamma_\rho Lv_b T_{\rho\sigma}(p_t + p_{\bar{b}}) \\ & \bar{v}_e\not{p}_{e^+}\not{p}_{\bar{b}}\gamma_\sigma Lv_{\nu_e}, \end{aligned} \quad (5)$$

$$\begin{aligned} \mathcal{M}_0^{(d)} = & -\frac{8i\sqrt{2\pi\alpha}M_W^2G_F}{2}G(p_t + p_{\bar{b}}; M_W) \\ & G(p_{e^+} - p_{\bar{\nu}}; M_W)\bar{u}_t\gamma_\rho Lv_b T_{\rho\sigma}(p_t + p_{\bar{b}}) \\ & [\epsilon_\mu \cdot (p_{e^+} - p_{\bar{\nu}} - p_\gamma)_\sigma + \epsilon_\sigma \cdot (p_t + p_{\bar{b}} + p_\gamma)_\mu \\ & - g_{\mu\sigma}(p_{e^+} - p_{\bar{\nu}} + p_t + p_{\bar{b}}) \cdot \epsilon] \\ & T_{\mu\lambda}(p_{e^+} - p_{\bar{\nu}})\bar{v}_e\gamma_\lambda Lv_{\nu_e}, \end{aligned} \quad (6)$$

with the propagator

$$G(p; M) \equiv \frac{1}{p^2 - M^2 + iM\Gamma}, \quad (7)$$

the tensor

$$T_{\rho\sigma}(p_i + p_j) \equiv g_{\rho\sigma} - \frac{(p_i + p_j)_{w\rho} \cdot (p_i + p_j)_{w\sigma}}{M_W^2}, \quad (8)$$

and $L \equiv \frac{1}{2}(1 - \gamma_5)$, $R \equiv \frac{1}{2}(1 + \gamma_5)$. In (7), M and Γ stand for the mass and decay width of the particle, respectively. The width term $iM\Gamma$ in (7) is important when p^2 is close to M^2 .

*There is a recent paper [17] studying single top quark production in $e\gamma$ collision at tree level in the SM and with the consideration of possible anomalous Wtb couplings but without considering the contributions from light PGB(s). Our present study is different from that in Ref. [17] by taking account of one-loop corrections and the light PGB(s) contributions which are shown to be significant.

The TC and top-color contributions to this process depends on the models. We take certain models as typical examples.

1. The TC2 Models

We first consider the TC2 model. There have been improvements of the TC2 model [9] to overcome some shortcomings of the original model and make it more realistic [21] [9]. Since the purpose of this paper is to test the characteristic effects of the charged PGB's, we are not considering the delicate refinements and shall simply take the original TC2 model (TOPCTC) [8] and the topcolor-assisted multiscale technicolor model (TOPCMTc) model [28] [15] [16] as typical examples.

a. The TOPCTC Model

In the TOPCTC model, there is a charged top-pion Π_t^+ in the top-color sector with mass around 200 GeV and decay constant $F_\pi^t = 50$ GeV [8]. We take its TC sector to be the standard ETC model, thus there is a charged technipion Π^+ from the TC sector with mass around 100 GeV and decay constant $F_\Pi = 123$ GeV [1]. As we have seen from Refs. [22] [16] that the TC and top-color gauge boson contributions to the Wtb vertex and the direct TC dynamics contribution to the $t\bar{t}$ production rate are only of the order of a few percent which are much smaller than the $t\bar{t}$ -channel PGB contributions to the top quark pair productions [15] [16]. Thus we concentrate our study to the PGB contributions in this paper.

The Feynman diagrams for PGB contributions to the process $e^+\gamma \rightarrow t\bar{b}\nu_e$ are shown in Fig. 1(e)-(r)[†]. Fig. 1(e)-(i) are the most important $t\bar{b}$ -channel PGB contributions[‡]. Our numerical results show that other diagrams [Fig. 1(j)-(r)] give much smaller contributions.

The technifermion triangle loop contribution to the $\Pi^+ - W^+ - \gamma$ vertex [Fig. 1(e)] in ETC models can be approximately evaluated [23] from the formulae for the Adler-Bell-Jackiw anomaly [24]. The result has been

[†]There are additional loop diagrams with the photon line attached to the PGB line and the external t and \bar{b} lines which vanish in the approximation $m_e \approx 0$ in our calculation, so that they are not shown in Fig. 1.

[‡]The triangle loops in Figs. 1(e)-(g) give rise to a large effective PGB- W - γ coupling, so that the contributions of these diagrams are sometimes regarded as effective tree-level contributions.

given in Ref. [25]. The $\Pi^+ - W^+ - \gamma$ coupling is:

$$\frac{S_{\Pi^+W^+\gamma}}{4\pi^2 F_\pi} \varepsilon_{\mu\nu\alpha\beta} \epsilon_1^\mu \epsilon_2^\nu k_1^\alpha k_2^\beta, \quad (9)$$

$$S_{\Pi^+W^+\gamma} = \frac{e^2}{2\sqrt{3}s_w} N_{TC}, \quad (10)$$

where the technicolor number is taken to be $N_{TC} = 4$.

The quark triangle loops [Fig. 1 (f)-(g)] are more complicated. They contain both the top quark and the bottom quark propagators with the masses of these quarks relatively light and significantly different. The contributions of these triangle loops are thus essentially different from the result of the Adler-Bell-Jackiw anomaly, and they actually contain logarithmic ultraviolet divergences. There are no corresponding tree-level terms to absorb these divergences. However, to guarantee $U(1)_{em}$ gauge invariance, we should also take account of Fig. 1(h)-(i) [nonvanishing as $m_e \approx 0$] which also contain logarithmic ultraviolet divergences, and cannot be absorbed into tree-level terms. Explicit results show that these two kinds of ultraviolet divergences just cancel each other and the total result is finite as it should be. This makes the charged channel $e^+\gamma \rightarrow t\bar{b}\nu_e$ very different from the neutral channel $\gamma\gamma \rightarrow t\bar{t}$.

To explicitly calculate the contributions of Fig. 1(f)-(i), we need the coupling of technipion Π and top-pion to quarks. In the original ETC models without top-color, the coupling of Π to quarks has been given in Ref. [25] which is

$$ic_f \frac{m_t}{F_\Pi} \bar{u}_t L u_b \Pi^+ + h.c. \quad (11)$$

Where, $c_f = \frac{1}{\sqrt{6}}$. In TC2 models, the ETC dynamics only provides a small part of the top quark mass m_t' . For reasonable range of the parameters in TC2 models, $m_t' \sim 5 - 20$ GeV [8] [26]. Thus the coupling of the technipion Π^+ to quarks in TC2 models can be obtained by replacing m_t by m_t' in (11), i.e.

$$ic_f \frac{m_t'}{F_\Pi} \bar{u}_t L u_b \Pi^+ + h.c. \quad (12)$$

Similarly, the coupling of the top-pion Π_t^+ to quarks is of the following form

$$i \frac{m_t - m_t'}{F_{\Pi_t}} \bar{u}_t L u_b \Pi_t^+ + h.c. \quad (13)$$

With (12) and (13) we can do the explicit calculation of the contributions of Fig. 1(f)-(i) to the amplitude. In the calculation, we take dimensional regularization and the on-shell renormalization scheme. The obtained amplitude with TC corrections is

$$\mathcal{M} = \mathcal{M}_0 + \Delta\mathcal{M}_{TC}^{(e)} + \Delta\mathcal{M}_{TC}^{(f-i)}(\Pi^+) \quad (14)$$

$$+ \Delta\mathcal{M}_{TC}^{(f-i)}(\Pi_t^+) + \Delta\mathcal{M}_{TC}^{(j-r)},$$

where the superscripts denote the corresponding Feynman diagrams in Fig. 1. The explicit formulae for $\Delta\mathcal{M}_{TC}^{(e)}$, $\Delta\mathcal{M}_{TC}^{(f-i)}(\Pi^+)$, and $\Delta\mathcal{M}_{TC}^{(f-i)}(\Pi_t^+)$ are

$$\Delta\mathcal{M}_{TC}^{(e)} = -c_f \frac{m'_t M_W S_{\Pi+W+\alpha}}{4\pi^2 F_\Pi^2} \sqrt{2\sqrt{2}G_F} \quad (15)$$

$$G(p_t + p_{\bar{b}}; M_\pi) G(p_{e^+} - p_{\bar{\nu}}; M_W)$$

$$\bar{u}_t L v_b \varepsilon^{\mu\nu\alpha\beta} \epsilon_\mu (p_\gamma)_\alpha (p_{e^+} - p_\nu)_\beta$$

$$T_{\mu\lambda} (p_{e^+} - p_{\bar{\nu}}) \bar{v}_e \gamma_\lambda L v_{\nu_e},$$

$$\Delta\mathcal{M}_{TC}^{(f-i)}(\Pi^+) = -ic_f \frac{m'_t M_W}{F_\Pi} \sqrt{2\sqrt{2}G_F} \quad (16)$$

$$G(p_t + p_{\bar{b}}; M_\Pi) G(p_{e^+} - p_{\bar{\nu}}; M_W) \bar{u}_t L v_b$$

$$\left[\Gamma_{\mu\nu}^{(f)}(\Pi) + \Gamma_{\mu\nu}^{(g)}(\Pi) + \Gamma_{\mu\nu}^{(h)}(\Pi) \right]$$

$$\epsilon_\nu T_{\mu\lambda} (p_{e^+} - p_{\bar{\nu}}) \bar{v}_e \gamma_\lambda L v_{\nu_e}$$

$$+ ic_f \frac{m'_t M_W}{F_\Pi} \sqrt{8\pi\sqrt{2}G_F \alpha}$$

$$G(p_t + p_{\bar{b}}; M_\Pi) G(p_t + p_{\bar{b}}; M_W) G(p_{e^+} + p_\gamma; 0)$$

$$\bar{u}_t L v_b [-i\Sigma_\mu(\Pi)] T_{\mu\nu} (p_t + p_{\bar{b}})$$

$$\bar{v}_e \not{\epsilon} (\not{p}_{e^+} + \not{p}_\gamma) \gamma_\nu L v_{\nu_e},$$

and

$$\Delta\mathcal{M}_{TC}^{(f-i)}(\Pi_t^+) = -i \frac{(m_t - m'_t) M_W}{F_{\Pi_t}} \sqrt{2\sqrt{2}G_F} \quad (17)$$

$$G(p_t + p_{\bar{b}}; M_{\Pi_t}) G(p_{e^+} - p_{\bar{\nu}}; M_W) \bar{u}_t L v_b$$

$$\left[\Gamma_{\mu\nu}^{(f)}(\Pi_t) + \Gamma_{\mu\nu}^{(g)}(\Pi_t) + \Gamma_{\mu\nu}^{(h)}(\Pi_t) \right] \epsilon_\nu$$

$$T_{\mu\lambda} (p_{e^+} - p_{\bar{\nu}}) \bar{v}_e \gamma_\lambda L v_{\nu_e}$$

$$+ i \frac{(m_t - m'_t) M_W}{F_{\Pi_t}} \sqrt{8\pi\sqrt{2}G_F \alpha} G(p_t + p_{\bar{b}}; M_{\Pi_t})$$

$$G(p_t + p_{\bar{b}}; M_W) G(p_{e^+} + p_\gamma; 0) \bar{u}_t L v_b$$

$$[-i\Sigma_\mu(\Pi_t)] T_{\mu\nu} (p_t + p_{\bar{b}}) \bar{v}_e \not{\epsilon} (\not{p}_{e^+} + \not{p}_\gamma) \gamma_\nu L v_{\nu_e}.$$

In (16)-(17) the functions $\Gamma_{\mu\nu}^{(f)}$, $\Gamma_{\mu\nu}^{(g)}$, $\Gamma_{\mu\nu}^{(h)}$, and Σ_μ are given in the Appendix in terms of the standard 2-point and 3-point functions B_0 , B_1 and C_0 , C_{ij} of the Feynman integrals [27]. The formula for $\Delta\mathcal{M}_{TC}^{(j-r)}$ is quite lengthy and we are not going to show it since its contribution is negligibly small compared with those shown in eqs.(15)-(17).

b. The TOPCMTC Model

The TOPCMTC model [28] [15] [16] differs from the TOPCTC model only on its ETC sector which is taken

to be the MWTC model [7]. In the TOPCMTC model, the main changes are: (a) the technipion Π^+ is almost composed of pure techniquarks [28], (b) the decay constant is $F_\Pi = 40$ GeV [7] rather than $F_\Pi = 123$ GeV in the usual ETC model. Thus the relevant changes in the above formulae are:

$$c_f = \frac{2}{\sqrt{6}}, \quad S_{\Pi+W+\gamma} = \frac{e^2}{4\sqrt{3}s_w}. \quad (18)$$

This change will enhance the Π^+ contribution [cf. eqs.(15)-(17)].

2. The Appelquist-Terning One Family ETC Model

This model is designed in which the techniquark sector respects the custodial $SU(2)$ symmetry, while the technilepton sector is custodial $SU(2)$ violating. The vacuum expectation value (VEV) F_Q of the techniquark condensate is much larger than the VEV F_L of the technilepton condensate [6]. There are 36 PGB's in this model, and the color singlet PGB's are mainly composed of technileptons which is irrelevant to the production of $t\bar{b}$. Thus in this model there are no $\Delta\mathcal{M}_{TC}^{(e)}(\Pi^+)$ and $\Delta\mathcal{M}_{TC}^{(f-i)}(\Pi^+)$. The only TC contribution to the $e^+\gamma \rightarrow t\bar{b}\bar{\nu}_e$ is $\Delta\mathcal{M}_{TC}^{(j-r)}$ which is much smaller than those in (15)-(17). Thus the cross sections in this model will be much smaller than those in the previous models.

We shall see from the numerical results in the next section that, for certain parameter range, these models can all be measured and distinguished by their $e^+\gamma \rightarrow t\bar{b}\bar{\nu}_e$ rates at the DESY TESLA.

III. THE CROSS SECTIONS

The hard photon beam of the $e^+\gamma$ collider can be obtained from laser backscattering at the e^+e^- linear collider [29]. Let \hat{s} and s be the center-of-mass energies of the $e^+\gamma$ and e^+e^- systems, respectively. After calculating the cross section $\sigma(\hat{s})$ for the subprocess $e^+\gamma \rightarrow t\bar{b}\bar{\nu}_e$, the total cross section at the e^+e^- linear collider can be obtained by folding $\sigma(\hat{s})$ with the photon distribution function $f_\gamma(x)$ ($\hat{s} = xs$)

$$\sigma_{tot} = \int_{(m_t+m_b)^2/s}^{x_{max}} dx \hat{\sigma}(\hat{s}) f_\gamma(x), \quad (19)$$

where

$$f_\gamma(x) = \frac{1}{D(\xi)} \left[1 - x + \frac{1}{1-x} - \frac{4x}{\xi(1-x)} + \frac{4x^2}{\xi^2(1-x)^2} \right], \quad (20)$$

with [29]

$$D(\xi) = \left(1 - \frac{4}{\xi} - \frac{8}{\xi^2} \right) \ln(1+\xi) + \frac{1}{2} + \frac{8}{\xi} - \frac{1}{2(1+\xi)^2}. \quad (21)$$

In (17) and (18), $\xi = 4E_e\omega_0/m_e^2$ in which m_e and E_e stand, respectively, for the incident electron mass and energy, ω_0 stands for the laser photon energy, and $x = \omega/E_e$ stands for the fraction of energy of the incident electron carried by the back-scattered photon. f_γ vanishes for $x > x_{max} = \omega_{max}/E_e = \xi/(1+\xi)$. In order to avoid the creation of e^+e^- pairs by the interaction of the incident and back-scattered photons, we require $\omega_0 x_{max} \leq m_e^2/E_e$ which implies that $\xi \leq 2+2\sqrt{2} \approx 4.8$. For the choice of $\xi = 4.8$, we obtain

$$x_{max} \approx 0.83, \quad D(\xi) \approx 1.8. \quad (22)$$

In the calculation of $\sigma(\hat{s})$, instead of calculating the square of the renormalized amplitude \mathcal{M} analytically, we calculate the amplitudes numerically by using the method of Ref. [30]. This greatly simplifies our calculations. Care must be taken in the calculation of the form factors expressed in terms of the standard loop integrals defined in Ref. [27]. As has been discussed in Ref. [31], the formulae for the form factors given in terms of the tensor loop integrals will be ill-defined when the scattering is forwards or backwards wherein the Gram determinants of some matrices vanish and thus their inverse do not exist. This problem can be solved by taking kinematic cuts on the rapidity y and the transverse momentum p_T . In this paper, we take

$$|y| < 2.5, \quad p_T > 20 \text{ GeV}. \quad (23)$$

The cuts will also increase the relative correction [32].

In our calculation, we take $m_t = 176 \text{ GeV}$, $m_b = 4.9 \text{ GeV}$, $M_W = 80.33 \text{ GeV}$, $G_F = 1.19347 \times 10^{-5} (\text{GeV})^{-2}$, $s_w^2 = 0.23$. The electromagnetic fine structure constant α at certain energy scale is calculated from the one-loop evolution formula with the boundary value $\alpha = 1/137.04$.

For the widths Γ of heavy particles appearing in (7), we take Γ_W to be 2.07 GeV [3] and Γ_t to be 7.5 GeV [11]. For the top-pion and technipion, when M_{Π_t} , $M_{\Pi} > m_t$, Π_t^+ and Π^+ decays dominantly into $t\bar{b}$. So, in this case

$$\Gamma_{\Pi_t} \approx \Gamma_{\Pi_t^+}(\Pi_t \rightarrow t\bar{b}) = \frac{(m_t - m_t')^2(m_{\Pi_t}^2 - m_t^2)^2}{16\pi F_{\Pi_t}^2 M_{\Pi_t}^3}. \quad (24)$$

$$\Gamma_{\Pi} \approx \Gamma_{\Pi^+}(\Pi \rightarrow t\bar{b}) = c_f^2 \frac{m_t'^2(m_{\Pi}^2 - m_t^2)^2}{16\pi F_{\Pi}^2 M_{\Pi}^3}. \quad (25)$$

When M_{Π_t} , $M_{\Pi} < m_t$, Π_t^+ and Π^+ decays dominantly into $c\bar{s}$. For small m_b , m_s , we approximately take Γ_{Π_t} and Γ_{Π} to be zero.

For estimating the event rates, we take the following integrated luminosities corresponding to a one-year-run at the DESY TESLA [33]

$$\begin{aligned} \sqrt{s} = 0.5 \text{ TeV} : \quad & \int \mathcal{L} dt \approx 500 \text{ fb}^{-1} \\ \sqrt{s} = 0.8 \text{ TeV} : \quad & \int \mathcal{L} dt = 500 \text{ fb}^{-1} \\ \sqrt{s} = 1.6 \text{ TeV} : \quad & \int \mathcal{L} dt \geq 500 \text{ fb}^{-1}. \end{aligned} \quad (26)$$

Our numerical results show that the contributions from the diagrams Figs. 1(j)-(r) to the production cross section are negligibly small in all models considered in this paper. Therefore we simply ignore them.

In the TOPTC model, the numerical results show that the TC PGB contributions to the production cross section are also negligibly small compared with the contributions from the top-pion. In Table 1, we list the correction to the production cross section $\Delta\sigma_{\Pi_t}$ (from the top-pion contributions) and the total cross section σ with $150 \text{ GeV} \leq m_{\Pi_t} \leq 350 \text{ GeV}$, $m_t' = 5, 20 \text{ GeV}$ at the 0.5 and 1.6 TeV LC. We see that the correction with $m_{\Pi_t} = 150 \text{ GeV}$ is significantly smaller than those with larger m_{Π_t} . This is due to the $t\bar{b}$ threshold effect in the Π_t resonance contribution. For $\sqrt{s} = 0.5 \text{ TeV}$, we see from Table 1 that the relative correction $\Delta\sigma_{\Pi_t}/\sigma_0$ is around 0.1% if m_{Π_t} is smaller than the threshold and around 3% if m_{Π_t} is larger than the threshold. For $\sqrt{s} = 1.6 \text{ TeV}$, $\Delta\sigma_{\Pi_t}/\sigma$ is around 0.2% if m_{Π_t} is smaller than the threshold and around 0.8% if m_{Π_t} is larger than the threshold. These TC PGB corrections are quite small compared with those in the neutral channel $\gamma\gamma \rightarrow t\bar{t}$ [16]. This is because that the contributions of Fig. 1(f)-(g) and Fig. 1(h)-(i) are destructive, which makes the charged channel very different from the neutral channel. With the integrated luminosity in (26), we see from the values of σ in Table 1 that, for a four-year run, there can be about ≈ 7000 events for $\sqrt{s} = 0.5 \text{ TeV}$, and ≥ 30000 events for $\sqrt{s} = 1.6 \text{ TeV}$. The corresponding statistical uncertainties at the 95% C.L. are then 2% for $\sqrt{s} = 0.5 \text{ TeV}$, and $\leq 1\%$ for $\sqrt{s} = 1.6 \text{ TeV}$. Thus the effect of the top-pion corrections can hardly be experimentally detected if m_{Π_t} is smaller than the threshold and for $\sqrt{s} = 1.6 \text{ TeV}$, but *can be marginally detected for $\sqrt{s} = 0.5 \text{ TeV}$ if m_{Π_t} is larger than the threshold* in

the sense of statistical uncertainty [§].

In the TOPCMTC model, the top-pion contributions are similar, while the Π^+ contributions are more significant than that in the TOPCTC model due to the smallness of F_Π in the TOPCMTC model. The numerical results in the TOPCMTC model are listed in Table 2 with the same ranges of m_{Π_t} and m'_t , and with $m_{\Pi^+} = 100$ and 250 GeV at the $\sqrt{s} = 0.5$ TeV and $\sqrt{s} = 1.6$ TeV LC. We see that the corrections are also significantly different for m_{Π^+} lying below or above the threshold. We see from Table 2 that the effect of Π^+ contributions, $\Delta\sigma_{\Pi^+}$, is negligibly small for $m_{\Pi^+} = 100$ GeV, while is quite significant for $m_{\Pi^+} = 250$ GeV. Take the $m'_t = 5$ GeV case as an example. For $m_{\Pi^+} = 250$ GeV, the relative correction $\Delta\sigma/\sigma$ ($\Delta\sigma \equiv \Delta\sigma_{\Pi_t} + \Delta\sigma_{\Pi^+}$) for $\sqrt{s} = 0.5$ TeV is around 20% and for $\sqrt{s} = 1.6$ TeV is around 5%, for m_{Π_t} smaller or larger than the threshold, i.e. the corrections are much larger in this model due to the Π^+ contributions. For $m_{\Pi^+} = 250$ GeV, the relative difference between the cross sections in the TOPCMTC model and the TOPCTC model $[\sigma(\text{TOPCMTC}) - \sigma(\text{TOPCTC})]/\sigma(\text{TOPCTC})$ is about 22% when $\sqrt{s} = 0.5$ TeV and about 5% when $\sqrt{s} = 1.6$ TeV. In this example, the number of events in a four-year run are about 8000 for $\sqrt{s} = 0.5$ TeV, and about 30000 for $\sqrt{s} = 1.6$ TeV. The corresponding statistical uncertainties at the 95% C.L. are then 2% for $\sqrt{s} = 0.5$ TeV and 1% for $\sqrt{s} = 1.6$ TeV. Thus the effect of the TC corrections in the TOPCMTC model can be clearly detected both at the $\sqrt{s} = 0.5$ TeV and $\sqrt{s} = 1.6$ TeV energies. The difference between the TOPCTC and TOPCMTC models can also be clearly detected at $\sqrt{s} = 0.5, 1.6$ TeV. So we conclude that *the TOPCTC and TOPCMTC models can even be experimentally distinguished at the $\sqrt{s} = 0.5, 1.6$ TeV TESLA via $e^+\gamma \rightarrow t\bar{b}\nu_e$ if m_{Π^+} is around 250 GeV.*

In the Appelquist-Terning one-family WTC model, the special arrangement of the F_Q and F_L causes that the color-singlet technipions are mainly composed of the technileptons, so that they do not couple to $t\bar{b}$. Thus there is no $t\bar{b}$ -channel PGB contribution to the production cross section, and the TC corrections are only from the diagrams in Figs. 1(j)-(r) which are negligibly small. Numerical calculation shows that the relative correction is smaller than 1%. So the effect of the TC corrections cannot be detected via the process $e^+\gamma \rightarrow t\bar{b}\nu_e$. This is significantly different from the

above TC models.

IV. CONCLUSIONS

In this paper, we have studied the possibility of testing different currently interesting improved technicolor models in the process $e^+\gamma \rightarrow t\bar{b}\nu_e$ at the $\sqrt{s} = 0.5$ TeV and $\sqrt{s} = 1.6$ TeV LC, especially the DESY TESLA, via the effects of their typical PGB's. We see that the $t\bar{b}$ -channel PGB contributions play dominant roles in this production process and their effects are experimentally detectable for certain reasonable parameter range in the sense of the statistical uncertainty. However, due to the destructive nature of the contributions of Fig. 1(f)-(g) and Fig. 1(h)-(i), the relative corrections in this charged channel are much smaller than those in the neutral channel $\gamma\gamma \rightarrow t\bar{t}$ [16], so that larger integrated luminosity is needed in the detection.

Specifically, in a four-year run of the DESY TESLA, the effects of the $t\bar{b}$ -channel PGB's in the TOPCTC, TOPCMTC models are all experimentally detectable for reasonable parameter range, and these models can be experimentally distinguished through the differences of their cross sections. The Appelquist-Terning model, as a typical example of models without a $t\bar{b}$ -channel PGB, is not detectable in the $e^+\gamma \rightarrow t\bar{b}\nu_e$ process at the LC. Thus the $e^+\gamma \rightarrow t\bar{b}\nu_e$ process at the LC provides a feasible test of the $t\bar{b}$ -channel charged PGB's in various TC models.

Since the recent Fermilab CDF data on $t\bar{t}$ production at the Fermilab Tevatron show that the branching fraction for a top quark decaying into a final state e or μ is consistent with the SM prediction [18], a charged top-pion lighter than the top quark seems to be disfavored [8], and a charged top-pion heavier than the top quark will have a broad width so that it is difficult to detect directly. Our results in the TOPCTC model shows that the $e^+\gamma \rightarrow t\bar{b}\nu_e$ process at the DESY TESLA provides feasible test of the charged top-pion effect.

ACKNOWLEDGMENTS

This work is supported by the National Natural Science Foundation of China, the Fundamental Research Foundation of Tsinghua University and a special grant from the State Commission of Education of China.

[§]A practical analysis of the detectability concerns also the systematic error and the detection efficiency in the experiments which is beyond the scope of this paper.

APPENDIX

Here we give the explicit expressions for $\Gamma_{\mu\nu}^{(f)}(\Pi)$, $\Gamma_{\mu\nu}^{(g)}(\Pi)$, $\Gamma_{\mu\nu}^{(h)}(\Pi)$, $\Sigma_\rho(\Pi)$, $\Gamma_{\mu\nu}^{(f)}(\Pi_t)$, $\Gamma_{\mu\nu}^{(g)}(\Pi_t)$, $\Gamma_{\mu\nu}^{(h)}(\Pi_t)$, and $\Sigma_\rho(\Pi_t)$ which can be obtained by direct calculations of the Feynman diagrams in Figs.1(g)-(i). The explicit expressions are

$$\begin{aligned} \Gamma_{\mu\nu}^{(f)}(\Pi) = & -c_f \frac{M_W m_t m'_t}{12\pi^2 F_\Pi} \sqrt{2\sqrt{2}\pi G_F \alpha_e} \{ 2[(p_{e^+} - p_{\bar{\nu}_e})_\mu \\ & (p_{e^+} - p_{\bar{\nu}_e})_\nu C_{21} + p_{\gamma\mu} p_{\gamma\nu} C_{22} + (p_{e^+} - p_{\bar{\nu}_e})_\mu p_{\gamma\nu} C_{23} \\ & + p_{\gamma\mu} (p_{e^+} - p_{\bar{\nu}_e})_\nu C_{23} + g_{\mu\nu} C_{24}] - g_{\mu\nu} B_0(p_\gamma, m_b, m_b) \\ & - g_{\mu\nu} m_t^2 C_0 + (2p_{e^+} - 2p_{\bar{\nu}_e} + p_\gamma)_\mu (p_{e^+} C_{11} - p_{\bar{\nu}_e} C_{11} \\ & + p_\gamma C_{12})_\nu + (p_{e^+} C_{11} - p_{\bar{\nu}_e} C_{11} + p_\gamma C_{12})_\mu (2p_{e^+} - 2p_{\bar{\nu}_e} + p_\gamma)_\nu \\ & - (p_{e^+} C_{11} - p_{\bar{\nu}_e} C_{11} + p_\gamma C_{12})^\rho (2p_{e^+} p_{\rho\mu\nu} - 2p_{\bar{\nu}_e} p_{\rho\mu\nu} \\ & + p_{\gamma\rho} g_{\mu\nu} + i\varepsilon_{\mu\rho\nu\sigma} p_\gamma^\sigma) + [2(p_{e^+} - p_{\bar{\nu}_e})_\mu (p_{e^+} - p_{\bar{\nu}_e})_\nu \\ & - (p_{e^+} - p_{\bar{\nu}_e})^2 g_{\mu\nu} + (p_{e^+} - p_{\bar{\nu}_e})_\mu p_{\gamma\nu} - g_{\mu\nu} p_{e^+} \cdot p_\gamma \\ & + g_{\mu\nu} p_{\bar{\nu}_e} \cdot p_\gamma + p_{\gamma\mu} (p_{e^+} - p_{\bar{\nu}_e})_\nu - i\varepsilon_{\mu\rho\nu\sigma} (p_{e^+} - p_{\bar{\nu}_e})^\rho \\ & p_\gamma^\sigma] C_0 \}, \end{aligned} \quad (A1)$$

$$\begin{aligned} \Gamma_{\mu\nu}^{(g)}(\Pi) = & c_f \frac{M_W m_t m'_t}{6\pi^2 F_\Pi} \sqrt{2\sqrt{2}\pi G_F \alpha_e} \{ 2[(p_{e^+} - p_{\bar{\nu}_e})_\mu \\ & (p_{e^+} - p_{\bar{\nu}_e})_\nu C_{21}^* + p_{\gamma\mu} p_{\gamma\nu} C_{22}^* + (p_{e^+} - p_{\bar{\nu}_e})_\mu p_{\gamma\nu} C_{23}^* \\ & + p_{\gamma\mu} (p_{e^+} - p_{\bar{\nu}_e})_\nu C_{23}^* + g_{\mu\nu} C_{24}^*] + (p_{e^+} C_{11}^* - p_{\bar{\nu}_e} C_{11}^* \\ & + p_\gamma C_{12}^*)_\mu (2p_{e^+} - 2p_{\bar{\nu}_e} + p_\gamma)_\nu - p_{\gamma\mu} (p_{e^+} C_{11}^* - p_{\bar{\nu}_e} C_{11}^* \\ & + p_\gamma C_{12}^*)_\nu + g_{\mu\nu} (p_{e^+} \cdot p_\gamma C_{11}^* - p_{\bar{\nu}_e} \cdot p_\gamma C_{11}^*) \\ & - i\varepsilon_{\mu\rho\sigma\nu} [(p_{e^+} - p_{\bar{\nu}_e}) C_{11}^* + p_\gamma C_{12}^*]^\rho p_\gamma^\sigma \}, \end{aligned} \quad (A2)$$

$$\Gamma_{\mu\nu}^{(h)} = c_f \frac{M_W m_t m'_t}{4\pi^2 F_\Pi} \sqrt{2\sqrt{2}\pi G_F \alpha_e}$$

$$\frac{B_1(p_t + p_{\bar{b}}, m_t, m_b) + B_0(p_t + p_{\bar{b}}, m_t, m_b)}{M_W^2}$$

$$\begin{aligned} & [(p_{e^+} - p_{\bar{\nu}_e})_\mu (p_{e^+} - p_{\bar{\nu}_e})_\nu - p_{\gamma\mu} p_{\gamma\nu} \\ & - g_{\mu\nu} (p_{e^+} - p_{\bar{\nu}_e})^2] \end{aligned} \quad (A3)$$

$$\begin{aligned} -i\Sigma_\mu(\Pi) = & c_f \frac{M_W m_t m'_t}{8\pi^2 F_\Pi} \sqrt{2\sqrt{2}\pi G_F} (p_t + p_{\bar{b}})_\mu \\ & [B_1(p_t + p_{\bar{b}}, m_t, m_b) + B_0(p_t + p_{\bar{b}}, m_t, m_b)] \end{aligned} \quad (A4)$$

$$\begin{aligned} C_{ij} = & C_{ij}(p_{\bar{\nu}_e} - p_{e^+}, -p_\gamma, m_t, m_b, m_b) \\ C_{ij}^* = & C_{ij}(p_{e^+} - p_{\bar{\nu}_e}, p_\gamma, m_b, m_t, m_t), \end{aligned} \quad (A5)$$

where C_{ij} 's are the standard 3-point functions given in Ref. [27].

The expressions for $\Gamma_{\mu\nu}^{(f)}(\Pi_t)$, $\Gamma_{\mu\nu}^{(g)}(\Pi_t)$, $\Gamma_{\mu\nu}^{(h)}(\Pi_t)$, and $\Sigma_\mu(\Pi_t)$ can be obtained by simply replacing m'_t by m_t - m'_t , F_Π by F_{Π_t} and taking $c_f = 1$.

-
- [1] S. Weinberg, Phys. Rev. D13, 974(1976); D19, 1277(1979); L. Susskind, Phys. Rev. D20, 2619(1979); S. Dimopoulos and L. Susskind, Nucl. Phys. B155, 237 (1979); E. Eichten and K. Lane, Phys. Lett. B90, 125 (1980).
 - [2] M. Peskin and T. Takeuchi, Phys. Rev. Lett. 65, 964 (1990).
 - [3] P. Langacker and J. Erler, hep-ph/9703428 (updated); and Phys. Rev. D54, 103 (1996).
 - [4] K. Hagiwara, D. Haidt, and S. Matsumoto, KEK Preprint KEK-TH-512, hep-ph/9706331.
 - [5] B. Holdom, Phys. Rev. D24, 1441 (1981); Phys. Lett. B150, 301 (1985); T. Appequist and L.C.R. Wijewardhana, Phys. Rev. D36, 568 (1987); K. Yamawaki, M. Banda and K. Matsumoto, Phys. Rev. Lett. 56, 1335 (1986); T. Akiba and T. Yanagida, Phys. Lett. B169, 432 (1986).
 - [6] T. Appelquist and J. Terning, Phys. Lett. B315, 139 (1993).
 - [7] K. Lane and E. Eichten, Phys. Lett. B222, 274 (1989); K. Lane and M.V. Ramana, Phys. Rev. D44, 2678 (1991).
 - [8] C.T. Hill, Phys. Lett. B345, 483 (1995);

- [9] K. Lane and E. Eichten, Phys. Lett. **B352**, 382 (1995); K. Lane, Phys. Rev. D**54**, 2204 (1996); k. Lane, Boston University Preprint BUHEP-97-8 (to appear in Proc. 1996 Workshop on Strongly Coupled Gauge Theories, Nagoya, Japan).
- [10] See for example, E.H. Simmons, R.S. Chivukula and J. Terning, in Proc. International Symposium on *Heavy Flavor and Electroweak Theory*, edited by C.-H. Chang and C.-S. Huang, Aug. 16-19, Beijing, China (World Scientific Pub., Singapore), pp.234-243.
- [11] CDF Collaboration, Phys. Rev. Lett. **72**, 2626 (1995); D0 Collaboration, Phys. Rev. Lett. **74**, 2632 (1995); L. Roberts, in Proc. of the 28th International conference on High Energy Physics, Warsaw, Poland, 1996.
- [12] For example, F. Larios and C.-P. Yuan, Phys. Rev. D**55**, 7218 (1997); F. Larios, E. Malkawi and C.-P. Yuan, in *Pysics at TeV Energy Scale* (CCAST-WL Workshop Series: Vol. 72), edited by Yu-Ping Kuang, July 15-26, 1996, CCAST, Beijing, China, pp.49-118.
- [13] For example, T. Han, K. Whisnant, B.-L. Young and X. Zhang, Phys. Lett. **B385**, 311 (1996); Phys. Rev. D**55**, 7241 (1997); M. Hosch, K. Whisnant and B.-L. Young, Iowa State Univ. Preprint AMES-HET-96-04; K.J. Abraham, K. Whisnant and B.-L. Young, AMES-HET-97-07; R.J. Oakes, K. Whisnant, J.M. Yang, B.-L. Young and X. Zhang, AMES-HET-97-08.
- [14] For example, J.M. Yang and C.S. Li, Phys. Rev. D**52**, 1541 (1995); C.H. Chang, C.S. Li, R.J. Oakes and J.M. Yang, Phys. Rev. D**51**, 2125 (1995); C.S. Li and J.M. Yang, in Proc. International Symposium on *Heavy Flavor and Electroweak Theory*, edited by C.-H. Chang and C.-S. Huang, Aug. 16-19, Beijing, China (World Scientific Pub., Singapore), pp.276-285 and references therein; C.S. Li, J.M. Yang, Y.L. Zhu and H.Y. Zhou, Phys. Rev. D**54**, 4662 (1996); H.Y. Zhou and C.S. Li, Phys. Rev. D**55**, 4421 (1996); C.S. Li, H.Y. Zhou, Y.L. Zhu and J.M. Yang, Phys. Lett. **B379**, 135 (1996); H. Wang, C.S. Li, H.Y. Zhou and Y.P. Kuang, Phys. Rev. D**54**, 4374 (1996).
- [15] E. Eichten and K. Lane, Phys. Lett. **B327**, 129 (1994); G. Mahlon and S. Parke, Phys. Rev. D**53**, 4886 (1996); S. Parke, in Proc. International Workshop on *Heavy Flavor and Electroweak Theory*, edited by C.-H. Chang and C.-S. Huang, Aug. 16-19, 1995, Beijing, China (World Scientific Pub., Singapore) pp. 273-275; C.-X. Yue, H.-Y. Zhou, Y.-P. Kuang and G.-R. Lu, Phys. Rev. D**55**, 5541 (1997).
- [16] H.-Y. Zhou, Y.-P. Kuang, C.-X. Yue, H. Wang and G.-R. Lu, Phys. Rev. D**57**, 4205 (1998).
- [17] E. Boos, A. Pukhov, M. Sachwitz and H.J. Schreiber, DESY Preprint DESY 97-123E, hep-ph/9711253.
- [18] F. Abe *et al.* (CDF Collaboration), Fermilab-Pub 97/286-E, hep-ph/9710008.
- [19] T. Stelzer and S. Willenbrock, hep-ph/9505433.
- [20] For example, R.S. Chivukula, S.B. Selipsky and E.H. Simmons, Phys. Rev. Lett. **69**, 575 (1992); R.S. Chivukula, E. Gates, E.H. Simmons and J. Terning, Phys. Lett. **B311**, 575 (1992); N. Evans, *ibid.* **331**, 378 (1994); E.H. Simmons, Boston Univ. Preprint BUHEP-96-37; C.-X. Yue, Y.-P. Kuang and G.-R. Lu, Phys. Rev. D**56**, 291 (1997); G.-R. Lu, Y.-G. Cao and X.-L. Wang, Phys. Rev. D**56**, 135 (1997).
- [21] R.S. Chivukula, B.A. Dobrescu and J. Terning, Phys. Lett. **B353**, 289 (1995); D. Kominis, Phys. Lett. **B358**, 312 (1995); G. Buchalla, G. Burdman, C.T. Hill and D. Kominis, Phys. Rev. D**53**, 5185 (1996).
- [22] Chong-Xing Yue, Yu-Ping Kuang and Gong-Ru Lu, Phys. Rev. D**56**, 291 (1997).
- [23] V. Lubicz and P. Santorelli, Nucl. Phys. **B460**, 3 (1996).
- [24] S. Adler, Phys. Rev. **177**, 2426 (1969); J.S. Bell and R. Jackiw, Nuo. Cim. **60A**, 47 (1969).
- [25] J. Ellis, M.K. Gaillard, D.V. Nanopoulos, and P. Sikivie, Nucl. Phys. **B182**, 529 (1981).
- [26] B. Balaji, Phys. Rev. D**53**, 1699 (1996).
- [27] G. Passarino and M. Veltman, Nucl. Phys. **B160**, 151 (1979); A. Axelrod, Nucl. Phys. **B209**, 349 (1982); M. Clements *et al.*, Phys. Rev. D**27**, 570 (1983).
- [28] K. Lane, Phys. Lett. **B357**, 624 (1995).
- [29] G. Jikia, Nucl. Phys. **B374**, 83 (1992).
- [30] K. Hagiwara and D. Zeppenfeld, Nucl. Phys. **B313**, 560(1989); V. Barger, T. Han and D. Zeppenfeld, Phys. Rev. **D41**, 2782(1990).
- [31] A. Denner, Fortschr. Phys. **41** 307(1994).
- [32] W. Beenakker *et al.*, Nucl. Phys. **B411**, 343(1994).
- [33] P.M. Zerwas, private communications.

TABLES

Table 1: Top-pion corrections to the $e^+\gamma \rightarrow t\bar{b}\nu_e$ production cross section $\Delta\sigma_{\Pi_t}$ and the total production cross section $\sigma = \sigma_0 + \Delta\sigma_{\Pi_t} + \Delta\sigma_{\Pi^+}$ in the TOPCTC models with $m_{\Pi^+} = 100$ GeV and various values of m_{Π_t} . The technipion corrections are negligibly small. The tree level production cross section $\sigma_0 = 3.25fb$ for $\sqrt{s} = 0.5\text{TeV}$, $\sigma_0 = 14.73fb$ for $\sqrt{s} = 1.6\text{TeV}$.

\sqrt{s} (TeV)	$m_t' = 5GeV$			$m_t' = 20GeV$		
	$m_{\Pi_t}(GeV)$	$\Delta\sigma_{\Pi_t}(fb)$	$\sigma(fb)$	$m_{\Pi_t}(GeV)$	$\Delta\sigma_{\Pi_t}(fb)$	$\sigma(fb)$
0.5	150	-0.003	3.25	150	-0.004	3.25
	200	0.084	3.33	200	0.065	3.32
	250	0.12	3.37	250	0.098	3.35
	300	0.10	3.35	300	0.087	3.34
	350	0.077	3.33	350	0.067	3.32
1.6	150	-0.13	14.60	150	-0.11	14.62
	200	0.053	14.78	200	0.032	14.70
	250	0.10	14.83	250	0.070	14.66
	300	0.13	14.86	300	0.097	14.72
	350	0.11	14.84	350	0.082	14.65

Table 2: Top-pion and technipion corrections to the $e^+\gamma \rightarrow t\bar{b}\nu_e$ production cross section $\Delta\sigma_{\Pi_t}, \Delta\sigma_{\Pi^+}$ in the TOPCMTC models with $\sqrt{s} = 0.5, 1.6\text{TeV}$ and various values of $m_{\Pi_t^+}, m_{\Pi^+}, m'_t$. The total production cross section $\sigma = \sigma_0 + \Delta\sigma_{\Pi_t} + \Delta\sigma_{\Pi^+}$. The tree level production cross section $\sigma_0 = 3.25\text{fb}$ for $\sqrt{s} = 0.5\text{TeV}$, $\sigma_0 = 14.73\text{fb}$ for $\sqrt{s} = 1.6\text{TeV}$.

\sqrt{s} (TeV)	m_{π^+} (GeV)	m_{π_t} (GeV)	$m'_t = 5\text{GeV}$			$m'_t = 20\text{GeV}$		
			$\Delta\sigma_{\Pi_t}(\text{fb})$	$\Delta\sigma_{\Pi^+}(\text{fb})$	$\sigma(\text{fb})$	$\Delta\sigma_{\Pi_t}(\text{fb})$	$\Delta\sigma_{\Pi^+}(\text{fb})$	$\sigma(\text{fb})$
0.5	100	150	-0.003	-0.00086	3.25	-0.004	-0.002	3.25
		200	0.084		3.33	0.065		3.32
		250	0.12		3.37	0.098		3.35
		300	0.10		3.35	0.087		3.34
		350	0.077		3.33	0.067		3.32
	250	150	-0.003	0.77	4.02	-0.004	3.12	6.37
		200	0.084		4.10	0.065		6.44
		250	0.12		4.14	0.098		6.47
		300	0.10		4.12	0.087		6.46
		350	0.077		4.10	0.067		6.44
1.6	100	150	-0.13	-0.047	14.55	-0.11	-0.16	14.46
		200	0.053		14.73	0.032		14.60
		250	0.10		14.78	0.070		14.64
		300	0.13		14.81	0.097		14.67
		350	0.11		14.79	0.082		14.65
	250	150	-0.13	0.71	15.31	-0.11	9.45	24.07
		200	0.053		15.49	0.032		24.21
		250	0.10		15.54	0.070		24.25
		300	0.13		15.57	0.097		24.28
		350	0.11		15.55	0.082		24.26

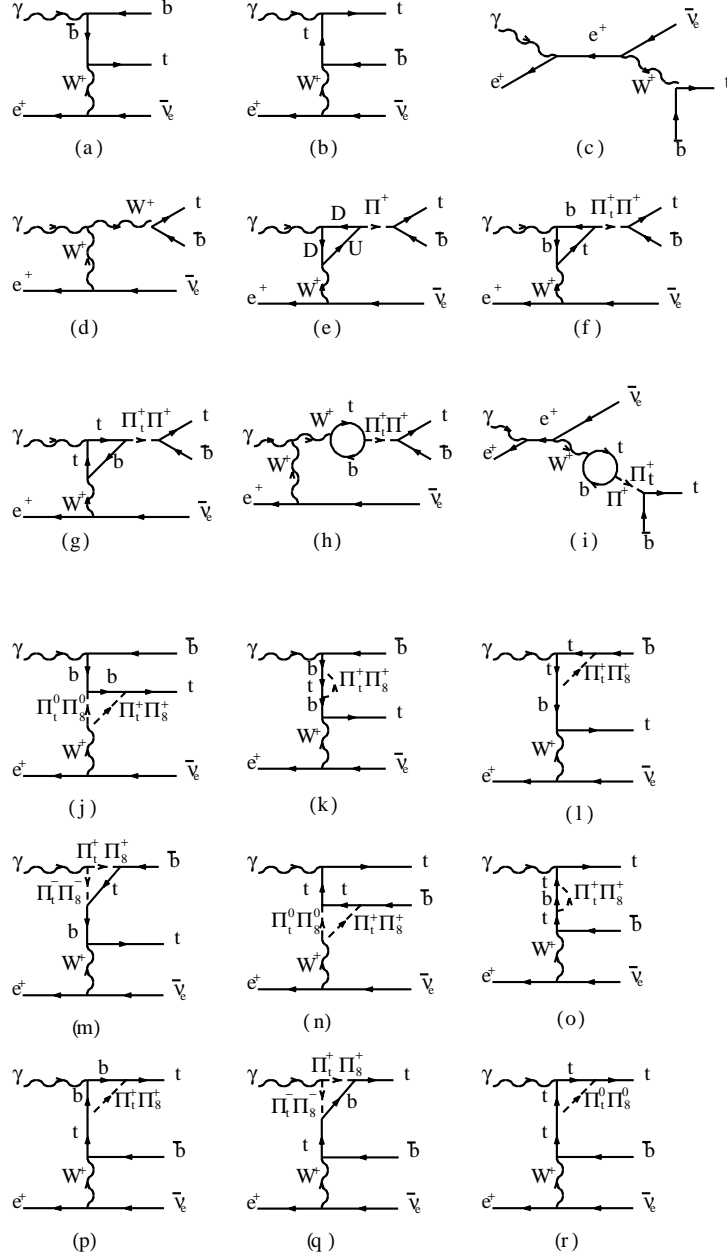


FIG. 1. Feynman diagrams contributing from various TC Models to the process $e^+ \gamma \rightarrow t \bar{b} \bar{\nu}_e$. The dashed lines denote color-singlet technipions or top-pions.